Molecular-field theory of the magnetic configurations and transverse magnetization processes in systems with high-order uniaxial anisotropy and strong antisymmetric exchange, with applications to some Sr-substituted hexagonal ferrites

M. Acquarone
Istituto di Fisica dell'Università, Gruppo Nazionale di Struttura della Materia del Consiglio Nazionale delle Ricerche, Parma, Italy

(Received 11 August 1980)

We study in the molecular-field approximation the equilibrium configuration and the phase transitions of a magnetic model system consisting of two sets of moments of equal magnitude, coupled by isotropic, anisotropic, and antisymmetric exchange, in the presence of uniaxial anisotropy, under the effect of a transverse magnetic field. The anisotropy is developed up to the sixth-order terms, with no restricting conditions upon the relative strength of the different interactions. Two possible interpretations of the model are developed: as a two-sublattice system, and as a quasicontinuous distribution of magnetic moments, exhibiting spiral magnetic structures. The theoretical results are then applied to the interpretation of the unusual magnetic structures, magnetization curves, and phase transitions observed in some Sr-substituted hexagonal ferrites of the Y and Z families, allowing an estimation of all the interaction parameters.

I. INTRODUCTION

We shall study, within the framework of a mean-field approach, the equilibrium configurations of, and the phase transitions induced by an external magnetic field in, a model system consisting of a set of magnetic moments of equal magnitude, arranged along a linear chain and coupled by next-neighbor isotropic, anisotropic, and antisymmetric exchange [the last one is also called Dzyaloshinski-Moriya (DM) interaction], in the presence of single-ion uniaxial anisotropy of hexagonal symmetry, developed up to sixth-order terms. The direction of the vector $\vec{D}$, representing the DM interaction, coincides with the crystallographic c axis (which is also the direction of the chain), while the field $\vec{H}$ is orthogonal to it. Choosing the z direction along the c axis, we then assume $\vec{D}=(0,0,D)$ and $\vec{H}=(H,0,0)$, and we write the anisotropy energy for a magnetic moment $\vec{m}_i$ in the form

$$E_i^{\mathrm{an}}=K_2\sin^2\theta_i+K_4\sin^4\theta_i+K_6\sin^6\theta_i \ .$$

θ_i is the angle between $\vec{m}_i$ and the c axis, and we neglect another possible sixth-order term, which would break the cylindrical symmetry, as no experimental evidence of it has been found in the materials we are interested in. The energy of two magnetic moments of unit length $\vec{m}_i$ and $\vec{m}_j$, coupled by the set of interactions considered above, can be written as follows:

$$E_{ij}=J_{ij}\vec{m}_i\cdot\vec{m}_j+K_z m_{iz}m_{jz}+\vec{D}_{ij}\cdot\vec{m}_i\times\vec{m}_j+K_2[(1-m_{iz}^2)+(1-m_{jz}^2)]$$
$$+K_4[(1-m_{iz}^2)^2+(1-m_{jz}^2)^2]+K_6[(1-m_{iz}^2)^3+(1-m_{jz}^2)^3]-\vec{H}\cdot(\vec{m}_i+\vec{m}_j) \ . \quad (1)$$

J_{ij} is the usual isotropic exchange, and K_z is the anisotropic exchange.

This model has more than a merely abstract interest: its complexity reflects the situation believed to exist in the hexagonal ferrites with the Y and Z structures.[1] In those materials, experimental evidence has been found for high-order terms in the anisotropy[2] and for a strong anisotropic exchange.[3] The antisymmetric exchange, allowed in particular crystal sites,[4] may have an enhanced effect when some substitution modifies some of the superexchange interaction paths, and lowers the crystal symmetry at well-defined sites.[5] This variety of interactions reflects itself in unusual magnetic structures and magnetization processes to be discussed in more detail in Sec. VII. Let us observe that Eq. (1) can be interpreted in a twofold way: if we put $i=1$ and $j=2$, it describes the coupling of two sublattice magnetizations, while if we put $j=i+1$, it describes the coupling of two neighboring moments along a chain. So the same formalism allows the study of both types of configurations observed by experiment.

Adding the DM interaction to a two-sublattice system with uniaxial anisotropy of hexagonal symmetry one is led to consider models analogous to those previously developed in connection with rhombohedral

systems, such as hematite[6,7] or Cr_2S_3.[8] The present study differs from the former ones in two respects: first, we do not introduce any simplifying assumption about the relative strength of the interactions, as, for instance, $J^2 >> D^2$. New magnetic configurations then appear, stable over a wide range of values of the interaction parameters and of the external field. Second, we develop the single-ion uniaxial anisotropy up to the sixth-order term. This is necessary since the results of previous work,[9,10] while confirming the relevant role of the DM interaction, demonstrated that lower order terms in the anisotropy failed to explain the observed transitions.

So the present study seems to be, with respect to the set of interactions considered, the most complete among the several papers published on two-sublattice semiclassical models.[6–8,10–13] Despite the complexity of the system, it is possible to give a rather transparent description of its equilibrium configurations, which include spiral, conical, axial, and planar structures. It is also possible to obtain precise information about allowed and forbidden phase transitions, and often to evaluate quantitatively the critical conditions as well. To arrive at these results, we use extensively the "root locus" technique, a powerful topological method to study high-order algebraic equations, developed in the context of control engineering over three decades ago, but practically unknown to the physicist.[14] The theoretical results are applied to the existing data, allowing for a quantitative evaluation of the interaction parameters.

To conclude, let us observe that the results presented in the following not only apply to materials other than Y and Z hexaferrites,[15] but also offer a useful classical reference frame to quantum-mechanical calculations about discrete Heisenberg magnetic chains,[16] which, in recent years have gone beyond simple isotropic exchange models to tackle more complicated situations as, for instance, an anisotropic exchange system in a transverse field,[17] or a chain of moments coupled by antisymmetric exchange.[18–20]

II. TWO-SUBLATTICE MODEL AND ITS EQUILIBRIUM EQUATIONS

To study the two-sublattice model, we transform Eq. (1) by introducing the usual ferro- and antiferromagnetic vectors $\vec{m}_+ \equiv \vec{m}_1 + \vec{m}_2$ and $\vec{m}_- \equiv \vec{m}_1 - \vec{m}_2$, and defining the following combinations of the physical parameters: $Z = \frac{1}{2}(J^2 + D^2)^{1/2}$, $\zeta = (K_z + J)/2$, $\beta = K_4/2$, $\gamma = 3K_6/16$. By substituting everything into Eq. (1), we obtain at last

$$E_{12} = (J/4)(m_{+x}^2 + m_{+y}^2 - m_{-x}^2 - m_{-y}^2) - \tfrac{1}{2}D(m_{+x}m_{-y} - m_{-x}m_{+y}) + \tfrac{1}{2}(K_2 + \zeta)m_{+z}^2$$
$$+\tfrac{1}{2}(K_2 - \zeta)m_{-z}^2 + \beta[4 + (m_{+z}^2 + m_{-z}^2)^2/4 - 2(m_{+z}^2 + m_{-z}^2) + m_{+z}^2 m_{-z}^2]$$
$$+(\gamma/6)(4 - m_{+z}^2 - m_{-z}^2[(4 - m_{+z}^2 - m_{-z}^2)^2 + 12m_{+z}^2 m_{-z}^2] + 2K_2 - Hm_{+x} \quad . \tag{2}$$

The vectors $\vec{m}_+$ and $\vec{m}_-$ are subject to two constraints, following the assumption $|\vec{m}_1| = |\vec{m}_2| = 1$: the orthogonality $\vec{m}_+ \cdot \vec{m}_- = 0$, and the normalization $|\vec{m}_+|^2 + |\vec{m}_-|^2 = 4$. Introducing two multipliers λ and μ one can define the Lagrange's functional L as

$$L = E_{12} + \lambda(|\vec{m}_+|^2 + |\vec{m}_-|^2 - 4) + \mu(\vec{m}_+ \cdot \vec{m}_-) \quad . \tag{3}$$

The equilibrium configurations of the system are those solutions of the set of equations $\partial L/\partial m_{nk} = 0$ ($n = +, -$; $k = x,y,z$), which also satisfy the constraints. The system of equations reads explicitly:

$$(4\lambda + J)m_{+x} + 2\mu m_{-x} - Dm_{-y} = 2H \quad , \tag{4}$$

$$2\mu m_{+x} + (4\lambda - J)m_{-x} + Dm_{+y} = 0 \quad , \tag{5}$$

$$Dm_{-x} + (4\lambda + J)m_{+y} + 2\mu m_{-y} = 0 \quad , \tag{6}$$

$$-Dm_{+x} + 2\mu m_{+y} + (4\lambda - J)m_{-y} = 0 \quad , \tag{7}$$

$$(2\lambda + K_2 + \zeta)m_{+z} + \mu m_{-z} = \beta m_{+z}(4 - m_{+z}^2 - 3m_{-z}^2) - \gamma m_{+z}(16 - 8m_{+z}^2 + m_{+z}^4) \quad , \tag{8}$$

$$\mu m_{+z} + (2\lambda + K_2 - \zeta)m_{-z} = \beta m_{-z}(4 - m_{-z}^2 - 3m_{+z}^2) - \gamma m_{-z}(16 - 8m_{-z}^2 + m_{-z}^4) \quad . \tag{9}$$

III. ZERO-FIELD CONFIGURATIONS AND THEIR STABILITY

In vanishing field, the system of Eqs. (9)–(14) allows for an explicit solution. We will class the possible configurations of stable equilibrium into five types: planar, ferro- and antiferromagnetic axial, ferro- and antiferromagnetic conical. In the following, quantities referring to the planar, conical, and axial structures will be labeled "p," "con," and "ax," respectively. To eliminate the degeneracy under rotation around the z direction in zero field, we choose $m_{+y}=0$ for all configurations, a choice which matches continuously the nonzero field solutions. The algebra is trivial, so we list only the final results in Table I, with a few comments. The components missing in the table vanish identically. The values for the nonplanar configurations of antiferromagnetic type can be obtained from the ferromagnetic ones just by changing the sign of ζ and interchanging m_{+z} with m_{-z}. The results for the conical structure are obtained with a $\pm$ in front of the square root of the quantity

$$R^2=\beta^2+4\gamma(Z+K_2+\zeta) \ .$$

However, one choice of the sign corresponds to an energy greater than the other one, so it can be discarded. In contrast to the other ones, the conical solutions are not possible for an arbitrary choice of the physical parameters, but only when the latter ones satisfy the inequalities following the requisites $R^2\geq 0$, $m_{+x}^2\geq 0$, and $0\leq m_{\pm z}^2\leq 4$. To discuss these conditions compactly it is useful to observe that the ferromagnetic solutions of any type are lower in energy than any antiferromagnetic one when $\zeta<0$ and vice versa, as can be seen from Eq. (1). Then we can write in an unified way the expressions for both magnetic symmetries if we substitute $-|\zeta|$ for ζ in the relations of Table I, so that the resulting expressions will be correct for the configuration lower in energy. Moreover, it is useful to introduce another combination of the interaction parameters $p\equiv Z+K_2-|\zeta|$. Then we can write the inequalities defining the existence conditions of the conical structures as follows:

$$R^2=\beta^2+4\gamma p\geq 0 \ , \quad 0\leq(-\beta+R)/8\gamma\leq 1 \ .$$

The results can be represented on a plane having p as abscissa and β as ordinate, for the two signs of γ. On the (p,β) plane the existence regions are then defined as follows: if $\gamma>0$ and $p<0$, then

$$p/4-4\gamma\leq\beta\leq-2(\gamma|p|)^{1/2} \ ;$$

if $\gamma>0$ and $p>0$, then

$$\beta\geq p/4-4\gamma \ ;$$

if $\gamma<0$, both p and β must be >0. In addition β must verify

$$\beta\geq 2(|\gamma|/p)^{1/2} \text{ if } 0\leq p\leq 16|\gamma| \ ,$$

$$\beta\geq p/4-4\gamma \text{ if } p>16|\gamma| \ .$$

We can now investigate in which regions of the (p,β) plane each of the equilibrium configurations realizes the absolute minimum of the energy. We obtain immediately $E^{\rm con}<E^{\rm ax}$ if $\beta/2+R>0$. A simple discussion shows that the conical phase is always lower in energy than the axial one in its own existence range, but for $p<0$ and $\gamma>0$, where β must obey $\beta<-4(|p|\gamma/3)^{1/2}$. The condition $E^{\rm p}<E^{\rm ax}$ is immediately written as $\beta<p/2-8\gamma/3$. The condition $E^{\rm con}<E^{\rm p}$ results in the following inequality

$$\beta\geq\tfrac{1}{2}p-8\gamma/3-\tfrac{1}{192}(\beta-R)(\beta+2R)/\gamma^2 \ .$$

For positive γ, where the conical phase is possible if $p>-16\gamma$, that inequality becomes an identity on

TABLE I. The zero-field solutions of Eqs. (9)–(14), and the corresponding values of the energy and of λ. The formulas for the antiferromagnetic solutions can be obtained from the corresponding ferromagnetic ones by changing the sign of ζ there, and interchanging m_{+z} with m_{-z}. R and Q indicate combinations of the interaction parameters as shown:
$R=[\beta^2+4\gamma(K_2+\zeta+Z)]^{1/2}$, $Q=(-\beta+R)/8\gamma$.

Type of configuration	$m_{+x}(0)$	$m_{-x}(0)$	$m_{+z}(0)$	$m_{-z}(0)$	Energy in vanishing field	$\lambda(0)$
Conical ferromagnetic	$[(2-J/Z)Q]^{1/2}$	$[(2+J/Z)Q]^{1/2}$	$2(1-Q)^{1/2}$	0.0	$2(K_2+\zeta)-(\beta-R)^2(\frac{1}{2}\beta+R)/24\gamma^2+2K_2$	$\frac{1}{2}Z$
Axial ferromagnetic	0.0	0.0	2.0	0.0	$2(K_2+\zeta)+2K_2$	$\frac{1}{2}(-K_2+\zeta)$
Planar	$(2-J/Z)^{1/2}$	$(2+J/Z)^{1/2}$	0.0	0.0	$-2Z+2K_2+4\beta+32\gamma/3$	$\frac{1}{2}Z$

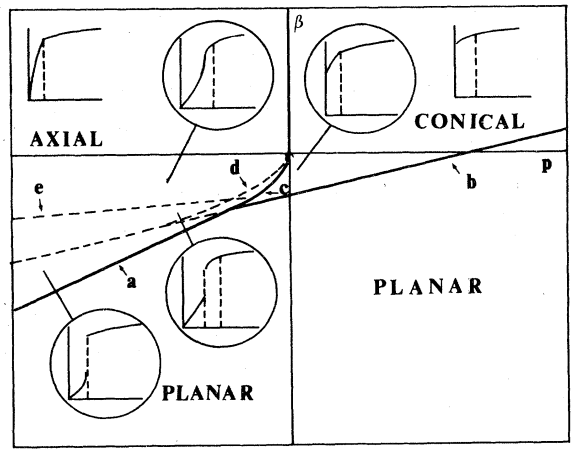

FIG. 1. Regions in the (p,β) plane corresponding to the existence and/or stability of the different configurations in vanishing field, for $\gamma > 0$. The boundaries of the regions (the lines labeled a, b, c, and d) are defined as follows: a: $\beta = \frac{1}{2}p - 8\gamma/3$, b: $\beta = p/4 - 4\gamma$, c: $\beta = -4(|p|\gamma/3)^{1/2}$, d: $\beta = -2(|p|\gamma)^{1/2}$. The line e: $\beta = p/16 - 4\gamma$ is defined and discussed in Appendix A. Also shown are the types of transverse magnetization curves one obtains if the interaction parameters fall in the regions corresponding to nonplanar configurations.

the lower border of the existence region ($\beta = p/4 - 4\gamma$). As the left side of the inequality above is a decreasing function of β, we conclude that $E^{\text{con}} < E^{\text{p}}$ in the whole existence region. For negative γ, a precise discussion requires a numerical evaluation. However, the exact boundary of the stability region is very well approximated by the two straight lines $\beta = p/2 - 8\gamma/3$ and $\beta = p/4 - 4\gamma$. The above discussion is visualized in Figs. 1 and 2.

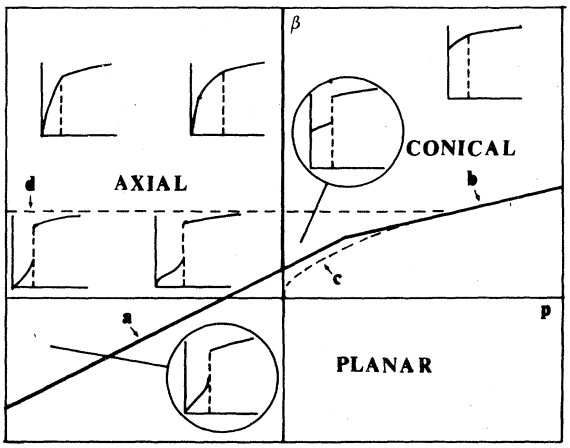

FIG. 2. Same as Fig. 1, but for $\gamma < 0$. The boundaries are defined as follows: a: $\beta = \frac{1}{2}p - 8\gamma/3$, b: $\beta = p/4 - 4\gamma$, c: $\beta = 2(|\gamma|p)^{1/2}$. The line d: $\beta = -8\gamma$ is discussed in the Appendix A.

IV. SOLUTION OF THE EQUILIBRIUM EQUATIONS FOR $H \neq 0$

Having retained only the sixth-order term with cylindrical symmetry in the anisotropy [another possible term having the structure $\sin^6\theta\cos 6(\psi_1 - \psi_2)$ could be present], the equilibrium equations for the in-plane components as functions of the Lagrange's multipliers, Eqs. (9)–(12), are decoupled from the equations for the z components, Eqs. (13) and (14), and have the following solution:

$$m_{+x} = \frac{H(4\lambda - J)}{2(4\lambda^2 - \mu^2 - Z^2)} , \tag{10}$$

$$m_{-x} = \frac{-H\mu}{(4\lambda^2 - \mu^2 - Z^2)} , \tag{11}$$

$$m_{+y} = 0 , \tag{12}$$

$$m_{-y} = \frac{HD}{(4\lambda^2 - \mu^2 - Z^2)} . \tag{13}$$

The configurations nonintrinsically unstable have $\mu = 0$, which means that the in-plane components of the magnetic moments $\vec{m}_1$ and $\vec{m}_2$ lay symmetrically with respect to the field direction, and that the z components have equal absolute values, as can be seen from the orthogonality relation. The relations above hold for any configuration: it is the difference in the values of λ, following the solution of the equations expressing the normalization and orthogonality constraints, which distinguishes the final form of the x and y components in the different configurations.

If we assume the identically vanishing solution for the Eqs. (8) and (9), to study the planar configuration, we arrive at an equation for λ which we write in the following form

$$1 - \frac{H^2}{16}\frac{(\lambda^2 - \frac{1}{2}\lambda J + Z^2/4)}{(\lambda^2 - Z^2/4)^2} = 0 . \tag{14}$$

This equation has been discussed in Ref. 9 (see also Ref. 21), and we recall here only the results of interest for what follows: the value of λ corresponding to a stable configuration is equal to (for $H = 0$) or greater than (for $H > 0$) $Z/2$, and the resultant m_{+x} is a strongly nonlinear function of H, as displayed in Fig. 3. If we consider Eq. (11) as an implicit equation for $\lambda(H)$, we can develop m^{p}_{+x} in powers of H, yielding

$$m^{\text{p}}_{+x} = m^{\text{p}}_{+x}(0) + \tfrac{1}{2}H/Z - (\tfrac{1}{2}H^2/Z^2)(2 - J/Z)^{1/2} + O(H^3) . \tag{15}$$

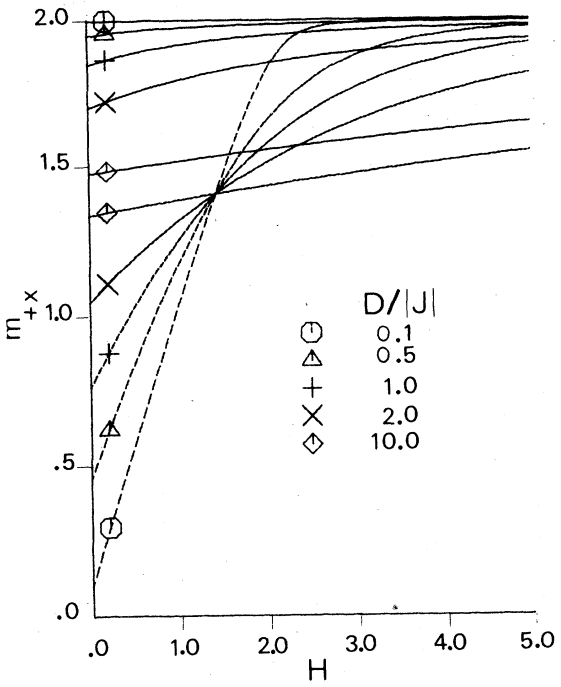

FIG. 3. Magnetization curves in the planar configuration for different values of D/J. Full line $J<0$; broken line $J>0$.

In discussing the nonplanar configurations, we keep the terminology of the preceding section, even if it is not to be taken literally here, because the configuration which we call "axial" here has nonvanishing in-plane components too, for $H\neq 0$. However, they must be kept distinguished, because it will turn out that the two configurations differ not only in the $H=0$ limit, but also for $H\neq 0$, for what concerns the behavior of the z-components. To simplify writing, let us introduce

$$t\equiv p-Z=K_2-|\zeta| \ . \tag{16}$$

The conical phases are characterized by $m_{\pm z}$ (according to their magnetic symmetry) given by

$$m^{con}_{\pm z}=2\left[1-\frac{-\beta+[\beta^2+4\gamma(2\lambda+t)]^{1/2}}{8\gamma}\right]^{1/2} . \tag{17}$$

The value of λ is fixed by the normalization equation, which reads

$$\frac{H^2(4\lambda^2-2\lambda J+Z^2)}{(4\lambda^2-Z^2)^2}+\frac{1}{2}\frac{\beta}{\gamma}=\frac{[\beta^2+4\gamma(2\lambda+t)]^{1/2}}{2\gamma} . \tag{18}$$

The axial configuration has the z components defined by an equation similar to, but not identical with Eq. (17). Indeed, it is no longer justified to consider only one sign in front of the root, as we did for the conical phase in discussing the zero-field formulas, as that reasoning, based on the expression of the energy corresponding to the conical configuration, is not applicable to the axial phase. To decide which of the two possibilities stemming from Eqs. (8) and (9), has to be chosen, we have to consider the zero-field limit of the z component itself. Introducing the appropriate value of λ from Table I we see that the requirement $\lim_{H\to 0} m^2_{\pm z}=4$ is met if we use the following expression, for any H value:

$$m^{ax}_{\pm z}=2\left[1-\frac{-\beta+(|\beta|/\beta)[\beta^2+4\gamma(2\lambda+t)]^{1/2}}{8\gamma}\right]^{1/2} . \tag{19}$$

When calculating the normalization equation from Eq. (19), we arrive at a relation analogous to Eq. (18), but possibly differing for the sign in front of the square root. However, to solve it, we square both sides, so that the final, ninth-degree equation for λ is one and the same for all nonplanar phases. Its coefficients $c_i (i=0,1,\ldots,9)$, listed according to decreasing powers of λ, are

$$\begin{aligned}
c_9&=512 \ ,\\
c_8&=256t \ ,\\
c_7&=-512Z^2 \ ,\\
c_6&=-256tZ^2-64\beta H^2 \ ,\\
c_5&=192Z^4+34\beta H^2 J \ ,\\
c_4&=96tZ^4+16\beta H^2Z^2-16\gamma H^4 \ ,\\
c_3&=-32Z^6+16\beta H^2JZ^2+16\gamma H^4J \ ,\\
c_2&=-16tZ^6+4\beta H^2Z^4-4\gamma H^4(J^2+2Z^2) \ ,\\
c_1&=2Z^8+2\beta H^2JZ^4+4\gamma H^4JZ^2 \ ,\\
c_0&=tZ^8-\beta H^2Z^6-\gamma Z^4H^4 \ .
\end{aligned} \tag{20}$$

Also for the nonplanar configurations it is possible to obtain from the characteristic equations the series development of the transverse magnetization, as follows:

$$m^{ax}_{+x}=-\frac{2t+J}{2(t^2-Z^2)}H+O(H^3) \ , \tag{21}$$

$$m^{con}_{+x}=m^{con}_{+x}(0)+\frac{1}{2}\frac{H}{Z}-\left[\frac{H^2}{4Z^2}\right]\times\left[\frac{2(2-J/Z)}{-\beta+[\beta^2+4\gamma(t+Z)]^{1/2}}\right]^{1/2}+O(H^3) \ . \tag{22}$$

V. PHASE TRANSITIONS BETWEEN EQUILIBRIUM CONFIGURATIONS

Due to the complexity of the model system, the study of the possible types of phase transitions

between different configurations can rarely go beyond the statement of necessary conditions relating a given transition to the values of the interaction parameters. We make use of the "root-locus" technique,[14] which proved very useful for studying simpler models,[9,10] even if, in the present case, new difficulties arise. Indeed, the coefficients c_i [see Eqs. (20)] do not depend linearly on any power of H, so that it is impossible to define a field-dependent "gain" for the locus. However, this technique is still the best tool

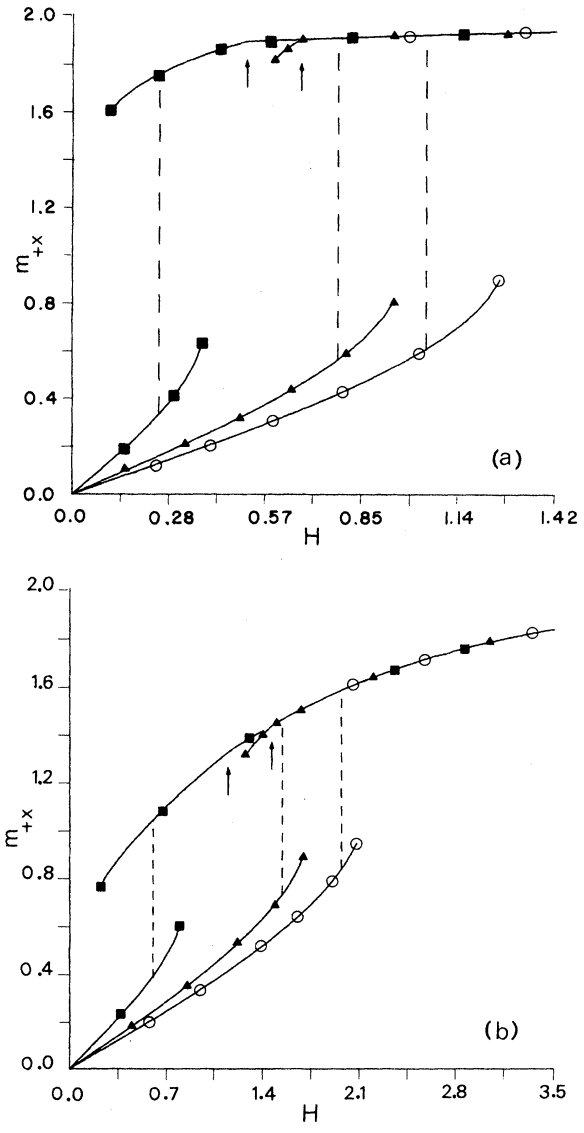

FIG. 4. Magnetization curves corresponding to the double phase transition for negative (a) and positive (b) values of J. Circles, triangles, and squares correspond, respectively, to situations where the conical phase is impossible, possible but metastable, and realized. The arrows indicate the second-order transition field.

one has to clarify to some extent the mathematical mechanisms underlying the transitions, and we exploit it as far as possible. The detailed discussion is rather lengthy, so we leave it for Appendix A, and report only the final results.

$\gamma < 0$: the transitions from any nonplanar configuration to the planar one are discontinuous whenever $\beta < -8\gamma$, and continuous otherwise; no transition between two nonplanar configurations is possible.

$\gamma > 0$: the conical-to-planar transition is always second order. The axial-to-planar transition cannot be a continuous one if $\beta < p/16 - 4\gamma$. That transition is a simple first-order one if $\beta < p/4 - 4\gamma$, but in the region $p/4 - 4\gamma < \beta < p/16 - 4\gamma$ there may be also a different process, by which the axial configuration has a discontinuous transition to a conical phase which, at a higher field, goes continuously into the planar configuration. This double transition is a typical feature of the present model, and is discussed in some detail in Appendix A. The exact boundaries of the region in the parameters plane where this process occurs could not be calculated explicitly, so that the values reported above guarantee the absence of the double transition, but should not be taken as the actual boundaries of its existence region. Examples of the latter type of transitions are shown in Fig. 4.

A panoramic view of the differently shaped magnetization curves calculated in different regions of the (p, β) plane, for both signs of γ, are displayed in Figs. 1 and 2. One sees that the curves transform in a continuous way under displacement on the plane, so that one can foresee rather accurately the shape in points different from those shown.

These results complete the study of the two-sublattice version of the model: in the next section we shall discuss briefly the continuous spiral structures.

VI. SPIRAL STRUCTURES

This kind of configurations has been studied in great detail in the case where it is a consequence of the coexistence of at least two competing superexchange interactions, coupling nearest and next-nearest neighbors, respectively.[22,23]

Without pretending here to give an exhaustive treatment of the problem, we show that also a DM term plus a single isotropic exchange, both coupling only nearest neighbors, can result in a spiral structure. We shall make some simplifying assumptions so that our results will strictly apply to the plane spiral only. However, due to the fact that we consider only the low-field situation, the resulting picture should not be too bad an approximation also for nonplanar arrangements. Introducing angular coordinates simplifies the calculation, so we define the turning angle at the site i along the chain (supposed of infinite length) as $\phi_i = \psi_{i+1} - \psi_i$, where ψ_i is the

angle between the projection of $\vec{m}_i$ on the basal plane and the direction of $\vec{H}$. If we assume $\theta_i = \theta_{i+1}$, the energy of two adjacent moments $E_{ij} = E_{i,i+1}$ can be written from Eq. (1) as

$$E_{i,i+1} = J\sin^2\theta_i\cos\phi_i - D\sin^2\theta_i\sin\phi_i + (J+k_z)\cos^2\theta_i + 2K_2\sin^2\theta_i + 2K_4\sin^4\theta_i + 2K_6\sin^6\theta_i - H[\cos\psi_i + \cos(\psi_i+\phi_i)]\sin\theta_i \quad . \tag{23}$$

The equilibrium value of θ_i is either $\pm\pi/2$ (corresponding to a plane spiral), or $n\pi$ ($n=0,1$ corresponding to the axial ferro- and antiferromagnetic arrangements) or a solution of

$$6K_6\sin^4\theta_i + 4K_4\sin^2\theta_i + 2K_2 - 2(J+K_z) + J\cos\phi_i - D\sin\phi_i = H[\cos\psi_i + \cos(\psi_i+\phi_i)] \quad . \tag{24}$$

To solve for ϕ_i the implicit equation $\partial E_{i,i+1}/\partial\phi_i = 0$, we pass from the discrete distribution of moments, defined only at the sites i spaced, say, by τ along the chain, to a continuous one, defined for every value of a continuous variable z. Starting from the identity

$$\phi_i = \tau(\psi_{i+1} - \psi_i)/(z_{i+1} - z_i)$$

we identify $(\psi_{i+1} - \psi_i)/(z_{i+1} - z_i)$ with $d\psi(z)/dz$ and we obtain (apart from an unphysical solution $\phi_i = \pm\pi/2$ at any field) the following differential equation:

$$\tau\frac{d\psi(z)}{dz} = \arctan\left[\frac{-D\sin\theta + H\sin\psi(z)}{J\sin\theta - H\cos\psi(z)}\right] \quad . \tag{25}$$

Since ϕ_i depends on i whenever $H \neq 0$, and θ_i depends on ϕ_i when the spiral is not a planar one, our assumption $\theta_i = \theta_{i+1}$, strictly speaking, is consistent only for $H = 0$, or for the plane spiral. The possible equilibrium arrangements and their stability conditions for the vanishing-field case bear, as is obvious, a close analogy to the results of Sec. III, so we will not repeat them here. We shall instead develop the study of the low-field case by ignoring the H dependence of θ: this, again, is correct only for the plane spiral. Equation (25) can be explicitly solved for $\psi = \psi(z)$, yielding the quantity of interest, the initial susceptibility $\chi = \lim_{H\to 0} dM(H)/dH$. We arrive at this value by developing $\cos\psi(z)$ up to first-order terms in H, and the integrating over a period. The final results are listed below, together with the upper value of the field for which the low-field solution is still acceptable (in a mathematical sense); we use $j \equiv J/D$ and $h \equiv H/D$.

(a) $j^2 >> 1$, $j < 0$

$$\chi = -1/2j, \quad h_c = 1 \quad . \tag{26}$$

(b) $j^2 >> 1$, $j > 0$

$$\chi = 1/[2j(\pi j - 1)], \quad h_c = (\pi j - 1)/(1+\pi^2)^{1/2} \quad . \tag{27}$$

(c) $j^2 << 1$, any sign of j

$$\chi = 1/(\pi + 2j), \quad h_c = (\pi + 2j)/(4+\pi^2)^{1/2} \quad . \tag{28}$$

In all cases the spiral structures obtained from this model show features analogs to those calculated by Enz[22] on a different model, namely, the existence of an upper critical field, and a linear rise of the magnetization in low fields. Of course, the details of the structures will be different, but they are indistinguishable by magnetization measurements only. However, these models are not to be taken literally in substituted hexaferrites, because one should expect the ideal infinite spiral to be broken into an ensemble of finite spirals of different length, so that a more realistic treatment should follow a monodimensional random-walk approach, the random variable being the length of each piece of spiral.

VII. COMPARISON WITH EXPERIMENTS ON Sr-SUBSTITUTED HEXAGONAL FERRITES OF *Y* AND *Z* TYPES

Let us recall that the crystals of the hexagonal ferrites may be built by stacking of chemical blocks (usually labeled S, T, and R for the Y and Z types) along the c axis.[1] Besides the crystallographic blocks, one can identify also magnetic blocks, possibly comprising several chemical blocks, as shown in Fig. 5. Inside each magnetic block, the localized spins stay mutually collinear, but the total magnetic moment of a block, acting as a single entity, may assume a canted orientation with respect to the moment of a contiguous block. If the interactions at the interface between magnetic blocks are such to sustain a noncollinear arrangement, in vanishing field the resulting configuration may be either a spiral (in or out of the plane orthogonal to the c axis), or an alternating structure, where each other moment is parallel, but contiguous moments form an angle both between themselves and with the c axis. In the litterature, the two types of configurations are termed "block conical spiral" and "block angular configuration," respectively. These "spiral" and "block angular" magnetic structures described in the Introduction have been observed, in a temperature range extending from 77 to 300 K, in samples of general composition $Ba_{2-x}Sr_xZn_2Fe_{12}O_{22}$ (Y type, usually shortened as $Ba_{2-x}Sr_xZn_2Y$) and $Ba_{3-x}Sr_xZn_2Fe_{24}O_{41}$ (Z type, usually shortened as $Ba_{3-x}Sr_xZn_2Z$) for several

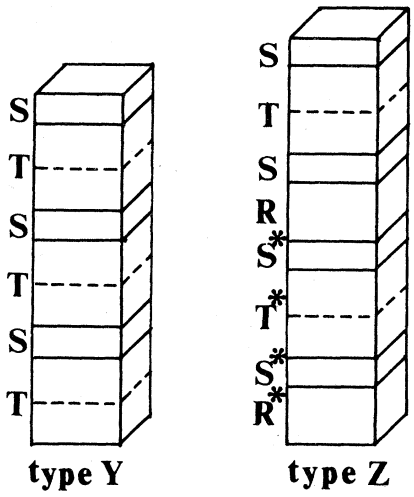

FIG. 5. Schematical representation (according to Ref. 1) of the crystallographic structure of the Y and Z hexagonal ferrites. The asterisk means that a block is rotated by 180° around the c axis. The broken lines mark the boundaries of the sections of the chemical cell which, by effect of substitution, act as a single magnetic unit.

values of x ; some evidence has also been found in Ba_2Mg_2Y.[5,24] To be more precise, the spiral has been detected by neutron diffraction in Y-type samples[25,26]: the moments always lay in or very near to the basal plane, and the spiral is stable for transverse fields lower than a few kOe. The alternating disposition has been observed, in vanishing field, only in the Z-type samples,[27] but it sets in also in Y-type samples for fields greater than a few kOe and not exceeding 15 kOe. If the latter value is exceeded, both systems go over to a canted planar configuration, slowly approaching complete parallelism in high fields. The changes of the magnetic structure show up also in the data on the transverse magnetization.[22,28–30] Steep rises in the transverse magnetization, separated by a rather flat plateau, mark the transition from the flat spiral to the nonplanar canted configuration, and from the latter to the canted planar one. The first transition appears clearly to be of first order, while the second one cannot be unambiguously classified from the published data. The same samples, in different temperature ranges, show more familiar magnetic configuration in vanishing field: an axial one (where all moments align ferro- or antiferromagnetically along the c axis), or a canted planar one. At high temperatures, the spontaneous configuration is always the planar arrangement; if the temperature is lowered, the appearance of the axial structure may, or may not precede the conical one, the sequence varying with the sample. Taking advantage from the fact that no such anomalies are observed in Zn_2Y and Zn_2Z containing only Ba, and that the substituting Sr ions are always localized in well-defined layers inside the T blocks for both structures, the starting point of a theory was the suggestion, first advanced by Enz,[22] that the substitution of Ba by Sr may result in a weakening of the superexchange interaction patterns across regularly spaced planes of the crystal. If any other interaction existed across the same planes, and was such to counteract the superexchange, a noncollinearity of blocks of spins, bounded by the substitution planes, may result.

Previous theoretical studies explored the effects either of competing superexchanges,[22] or of second-order uniaxial anisotropy assumed to dominate over the weakened superexchange.[29] The results obtained by both approaches are not free from criticism. First of all, none of them is comprehensive of both types of crystals, as the spiral model cannot describe the two-sublattice behavior, as observed in Z samples, while the other one cannot be applied to the spiral configurations. Moreover, they also offer separate reasons for criticism. According to Ref. 22, the plateau of the magnetization curve corresponds to an "oscillatory" structure existing up to a field whose value is about twice the field value at which the spiral disappears. Experimentally the former field is an order of magnitude greater than the latter. Moreover, the predicted and observed variations of the spatial period with increasing H appreciably disagree.[25,26,31] The susceptibility of the "oscillatory" phase, also, as calculated in Ref. 32, is much greater than measured. Finally, according to[23,32] the "oscillatory" phase always has a second-order transition to the ferromagnetic configuration stable in high fields, while, at least in some cases the observed transition appears to be a discontinuous one (see Fig. 6).

The picture emerging from the neutron data cited above is that, for values of H corresponding to the magnetization plateau, the moments along the ideal chain order symmetrically, alternating on the two sides of the direction of H.[33] It is then adequate to describe the overall structure as composed by two canted "supersublattices." A two sublattice approach is indeed adopted in Ref. 29, but the results reproduce the qualitative behavior of the data only if one assumes different values both for the magnetic moments, and for the anisotropy constants, of the sublattices. This is unlikely to be the case: indeed, the diamagnetic substitution affects a plane which divides the unit cell into identical halves. One cannot easily see which should be then the origin of the large physical differences postulated by this approach. Moreover, no spiral structures are possible, and the system exhibits a vanishing susceptibility in the plateau and in the planar configuration.

To improve the theory, one can take into account that the substitution has a qualitative, as well as a quantitative effect on the interactions. Indeed, by destroying a center of symmetry inside the T blocks,

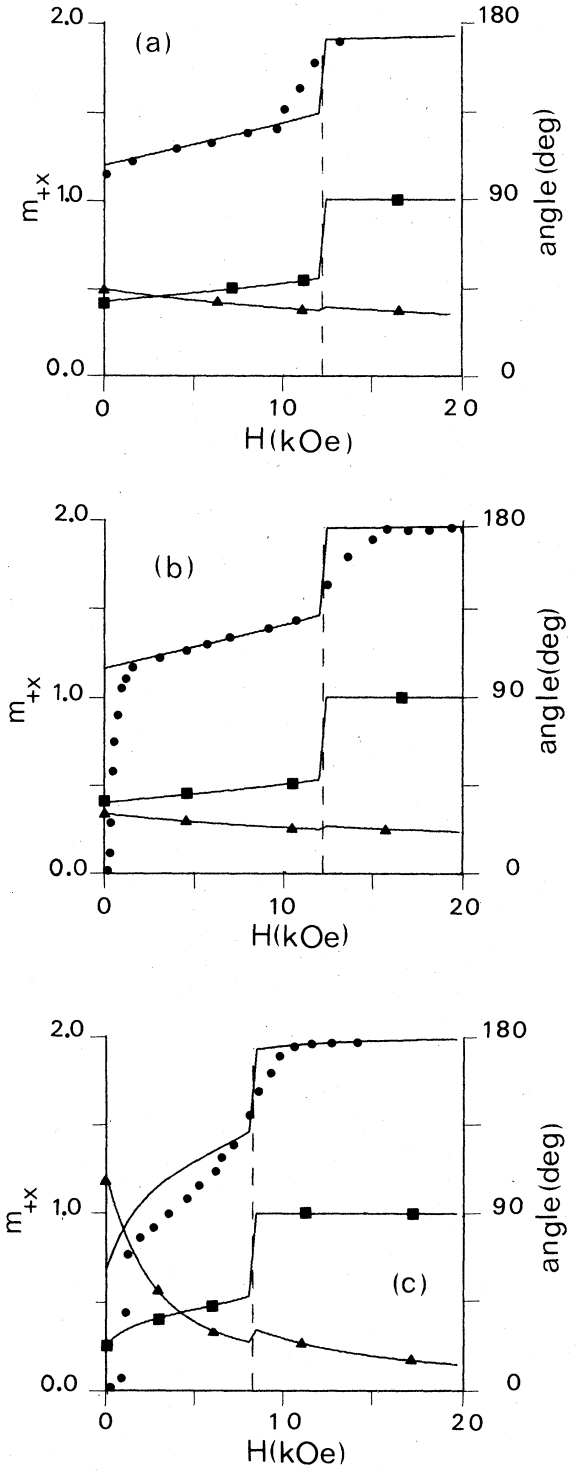

FIG. 6. Magnetization curves obtained from the theory, and the corresponding behavior of the angle ϕ (triangles) and of the direction of the resulting overall magnetization (squares). Diagrams labeled (a), (b), (c) are in correspondence with the lines of Table IV from top to bottom. The dots are the experimental values of the magnetization.

it opens the way to the action of the antisymmetric exchange (Refs. 4 and 5), so that the model discussed above is adequate to represent the physical situation.

The available data about the samples of interest concern magnetization and angle values. The measured angles are ϕ (the turning angle of the plane spiral and/or the angle between the in-plane projections of the two sublattice magnetic moments), and the angle between the easy magnetization direction and the c axis. The data set is not always a consistent one: for instance, there is some contradiction between the magnetization and the angle measurements of Ref. 29. Moreover, there seems to be a misunderstanding of the physical situation in the discussion of some neutron measurements.[25,26] For these reasons we decided to concentrate mainly on the fit to the magnetization, which represent an almost continuous (and self-consistent) set of data, as a function of the field, at a given temperature. By contrast, the angles constitute a scattered set of a few values. When the agreement with the magnetization data was rather good for more than one set of values of the interaction parameters, we used what appeared to be the most reliable value of ϕ to choose between the different possibilities.

The J/D ratio could in principle be obtained from three sources. One is the value of ϕ at vanishing H, and it is important to notice that both in the spiral and in the two-sublattice configurations, ϕ at $H=0$ has the same value. In the latter case, it has to be calculated as follows:

$$\phi = \arccos[(m_{+x}^2 - m_{-y}^2)/(m_{+x}^2 + m_{-y}^2)]$$
$$= \arccos[-j/(j^2+1)^{1/2}] \ ,$$

where $j \equiv J/D$. The values so obtained are listed in Table II. The other two sources are the initial susceptibility of the spiral configuration, and the value of the critical field at which the spiral disappears. In these two cases, a self-consistency check has to be made because the $H \neq 0$ results of Sec. II imply a definite assumption about the order of magnitude and the sign of J/D. Unfortunately, the susceptibility in the spiral phase can be clearly inferred from the data only in one case.[25] Moreover, as discussed in Sec. VI, those calculations cannot be supposed to have a quantitative meaning, because of the unrealistic assumptions of an infinite length of the spiral. Then, even the values of the fields at which the two-sublattice type of configuration sets in cannot be used to obtain reliable values of J/D.

Then the only practical source for estimating J/D was $\phi(0)$. When this value was not available, we estimated it by linearly extrapolating to $H=0$ the low-field magnetization plateau, and used the easy magnetization angle (EMA) value at $H=0$ to determine trigonometrically $\phi(0)$. Having so obtained an orientative value of J/D, we allowed the EMA at $H=0$

TABLE II. Some values of J/D as obtained from zero-field measurements of ϕ.

Compound	Type	T (K)	$\phi(H=0)$	J/D	Ref.
$Ba_{0.6}Sr_{2.4}Zn_2Fe_{24}O_{41}$	Z	77	45°	−1.0	27
$Ba_{0.6}Sr_{2.4}Zn_2Fe_{24}O_{41}$	Z	293	120°	0.575	27
$Ba_{0.4}Sr_{1.6}Zn_2Fe_{12}O_{22}$	Y	77	90°	0.0	26
$Ba_{0.4}Sr_{1.6}Zn_2Fe_{12}O_{22}$	Y	293	120°	0.575	26
$Ba_{0.4}Sr_{1.6}Zn_2Fe_{12}O_{22}$	Y	360	168°	4.87	26

value to vary at the end of the fit, to see if the overall agreement with the magnetization curves could be better. To fix separately J and D, we considered also the value of m_{+x} at some point in the planar configuration. Due to the very small difference with the saturation value, the values obtained are largely questionable. In general, one can say that the present theory would require much more precise data than are available.

The anisotropy parameters are linked through $m_{\pm z}(0)$ which depends on the value of $\theta_0=\theta(0)$. One has

$$\beta = p/(4\sin^2\theta_0) - 4\gamma\sin^2\theta_0 \ .$$

Further relations can be worked out after the nature of the passage from the conical to the planar arrangement is clarified. From some magnetization data one could guess that one is observing two continuous transitions: from conical (the plateau) to axial (the steep rise) to the planar configuration (second plateau). But our study of the root loci, in Sec. V, excludes this sequence of transitions. So what one sees must simply be a single transition from a conical to a planar configuration. No data are available to allow an unambiguous determination of its order, nor of the critical field value. We must then discuss two hypotheses: (a) a first-order transition blurred by experimental effects (for example, the coexistence of different domains, as discussed in Ref. 26); (b) a second-order transition, whose critical field should be at the end of the flat plateau, as the conical configuration does not give magnetization curves with an upward curvature (see the m_{+x} development, at the end of Sec. VI). In this hypothesis, the slope of the magnetization curve in the planar configuration appears greater than in the conical one. It is not difficult to calculate

$$\Delta\chi_c = \lim_{H\to H_c}\left(\frac{dm_{+x}^{\rm np}}{dH} - \frac{dm_{+x}^{\rm p}}{dH}\right)$$

for any nonplanar ("np") configurations. The discussion of the result, which is developed in Appendix B, shows that $\Delta\chi_c$ is always positive, implying that the only acceptable interpretation is a first-order transition. The sought for conditions on the anisotropy parameters follow from the discussion of the Sec. V:

(a) $\gamma<0$,

(b) $0<p<-16\gamma$,

(c) $-8\gamma>\beta>p/2-8\gamma/3$ if $0<p-16\gamma/3$,

$-8\gamma>\beta>p/4-4\gamma$ if $-16\gamma/3>p$.

One further condition can be worked out by considering the magnetization along the z axis in vanishing field. In samples with the spiral configuration one observes $m_{+z}(0)=0$, meaning that the configuration is either planar or axially antiferromagnetic. The former possibility can be ruled out because in vanishing fields the stability conditions of the spiral structures are analogous to those of the two-sublattice model configurations, and we find a nonplanar two-sublattice phase after the low-field transition. Then we can assume $\zeta>0$ in those compounds: this implies $K_z<|J|$ if $J<0$ and $|K_z|<J$ if $J>0$, together with $K_z<0$. In Z-type samples, exhibiting the two-sublattice conical configuration at $H=0$,[11] one has $m_{+z}(0)\neq 0$, implying $\zeta<0$ and $K_z<-J$ if $J>0$, or $|K_z|<|J|$ if $J<0$, together with $K_z>0$. However, K_z has a negligible influence on the calculated magnetization curves. As some measurements indicate[3] it to be of the same order of magnitude of K_2, we took $|K_z|=|K_2$. Figure 6 shows some of the theoretical curves fitted to magnetization measurements showing the conical phase. It is important to realize that the "theoretical" appearance of the curves is different from the experimental one. This is shown in Table III where the salient features of the curves are listed both in experimental units, and in the reduced "theoretical" units. One sees, for example, that the samples of Refs. 28 and 29 yield almost the same "theoretical" curve. The main difference is that the Z-type sample keeps a two-sublattice structure down to $H=0$. This confirms that the origin of their "strange" behavior must lay in a block common to both crystal structures, as is the case of the T block (see Fig. 5). That is the reason for which we do not show a separate fit for the sample of Ref. 29.

TABLE III. The measured values of the reduced magnetization and of the external field corresponding to the extreme of clearly identified sections of magnetization versus field curves showing evidence of the conical configuration. The field values with the suffix "e" are the experimental values (in kOe); the field values without suffix are the "theoretical" ones: $H_i = H_i^e/M_s$ ($i = 1, 2, 3$). The labels 1 and 2 correspond, respectively, to the lowest and highest fields for which the conical phase surely exists [except in the first line, where H_1 was chosen equal to the values in the second line to stress the similarity in the corresponding values of $m_{+x}(H_1)$]. The label 3 indicates the lowest field at which the planar phase is clearly established. M_s is in gauss.

Type	M_s	H_1^e	H_1	$m_{+x}(H_1)$	H_2^e	H_2	$m_{+x}(H_2)$	H_3^e	H_3	$m_{+x}(H_3)$	T (K)	Ref.
Z	430	2.696	6.27	1.244	9.72	22.60	1.408	13.64	31.72	1.866	77	29
Y	426	2.67	6.27	1.310	10.0	23.47	1.380	14.67	34.44	1.862	77	28
Y	282	0.870	3.085	0.790	6.52	23.13	1.368	10.87	38.55	1.994	293	25
Y	393	1.587	4.04	1.454	8.414	21.41	1.590	17.46	44.43	1.990	77	22
Y	269	1.526	5.67	1.162	10.0	31.17	1.420	15.0	55.76	1.960	200	22

We did not try any determination of the temperature variation of the interaction parameters in a given sample for two reasons. The main one is that we have no theory of the temperature variation of D. The second one is that, to fit the anisotropy constants in the hexaferrites by the theory of Ref. 34 one needs to know the temperature dependence of the magnetization of the sublattice responsible for the anisotropy.[35] Now, in the materials of interest one can neither determine which sublattice is responsible for the anisotropy, nor fully resolve the individual sublattice magnetization curves.[36]

The values of the interaction parameters given in Table IV are just orientative, because also other sets of values could, in general, fit the data as well. The theory in itself is rather sensitive to each individual parameter, but the available data are not precise enough. Some very important quantities, as the critical field for the first-order transition, can be read only with an error of, say, 30%, from the measurements. Others, as for instance, the variation of the z components with the field, have not been measured. From Table IV one sees that the magnetization curves themselves are similar for different sets of parameters (compare the first two lines), while the angles are much more sensitive to the precise values of the interactions. So one would need fully reliable measurements of the latter quantities to deduce unequivocally the parameters.

On the whole, the general agreement with the measurements seems satisfying, taking into account the internal inconsistencies and imprecisions of the data set discussed above.

One must, however, recognize that the fit with the $\theta(0)$ values is good only for the case where the zero-field structure is of the two-sublattice type.

TABLE IV. Values obtained by fitting the present theory to the data for some cases among those of Table III. H_c (in kOe) is the first-order transition field; $m_{+x}(H_c)$ refers to the conical configuration. The angle that the resulting overall magnetization forms with the c axis for $H = 0$ is indicated as EMA (easy magnetization angle). The interaction parameters are expressed in units of 10^6 erg/cm^3. K_z is shown between brackets below the K_2 value.

Ref.	Type	T (K)	$m_{+x}(H_1)$	$m_{+x}(H_2)$	H_c	$m_{+x}(H_c)$	$m_{+x}(H_3)$	$\phi(0)$	EMA	J	D	$K_2(K_z)$	K_4	K_6
29	Z	77	1.250	1.424	12.22	1.474	1.90	45°	58°	−7.30	7.30	15.86 ($-K_2$)	28.53	−13.33
22	Y	200	1.180	1.400	12.22	1.470	1.95	29°	36°	−5.29	3.11	5.92 (K_2)	16.34	−8.0
28	Y	293	0.790	1.356	8.0	1.450	1.95	108°	22°	0.213	0.61	8.53 (K_2)	8.64	−4.27

ACKNOWLEDGMENTS

The author wishes to thank Professor G. Asti and Dr. S. Rinaldi for constant interest and stimulating discussions, and Professor G. Albanese and Dr. A. Deriu for useful comments.

APPENDIX A: MATHEMATICS OF THE PHASE TRANSITIONS

It is better to postpone the examination of the root locus until we have worked out by a more usual approach some mathematically necessary conditions relating the interaction parameters to each type of transition. More stringent conditions on the parameters, and other possible phase transitions will appear from a root locus study of Eqs. (14) and (18), so justifying the use of that technique.

A second-order transition from a nonplanar to a planar configuration can take place if λ reaches a value λ_c such that $m_{\pm z}=0$. From Eqs. (17) and (19) this implies

$$8\gamma+\beta=\epsilon[\beta^2+4\gamma(2\lambda_c+t)]^{1/2} \ , \tag{A1}$$

$\epsilon=1$ for the conical configuration, and $\epsilon=|\beta|/\beta$ for the axial one. The only requisite on the parameters following the above equation is that both sides have the same sign, meaning that the axial-to-planar transition is surely first order when β satisfies the following inequalities:

$$\text{if } \gamma>0 \text{ then } -8\gamma<\beta<0 \ , \tag{A2a}$$

$$\text{if } \gamma<0 \text{ then } 0<\beta<-8\gamma \ . \tag{A2b}$$

The conical-to-planar transition is surely first order, instead, if

$$\beta<-8\gamma \tag{A2c}$$

for any γ. The value of λ_c for a second-order transition can be obtained from the equation above and it is:

$$\lambda_c=-t/2+2\beta+8\gamma \ .$$

The critical field, H_c, can then be obtained from Eq. (14), by substituting λ_c. The relations *a*, *b*, *c* allow for a transparent interpretation in terms of the topology of the root loci of Eq. (20). The best we can do to obtain a manageable form of Eq. (20), is to write it as follows:

$$1-\frac{\beta^2}{8\gamma}\frac{(\lambda^2-Z^2/4)^2+(\gamma/8\beta)H^2(4\lambda^2-2\lambda J+Z^2)^2}{(\lambda^2-Z^2/4)^2(\lambda+\frac{1}{2}t+\beta^2/8\gamma)}=0 \ . \tag{A3}$$

This is a very unorthodox root-locus equation, because the "gain" parameter $\beta^2/8\gamma$ also influences the value of the simple pole $P_1=-t/2-\beta^2/8\gamma$. Moreover, the zeros depend on H, so that to follow the effect of a varying field on the roots of Eq. (20), requires one to follow the evolution of an infinite ensemble of root loci, whose zeros move in the complex plane. This opens the way to the possibility of discontinuous relevant changes in the topology of the locus, generated by an infinitesimal change in the value of the external field. Indeed, it is the relative position of the poles (which depend here only on the interaction parameters and not on the field) and of the zeros (depending also on the latter) which essentially determines the topology of the locus. As a general consequence, we cannot expect that the position of a given root change continuously with the field in every instance. It will be shown in the following that precisely this topological discontinuity allows a quite peculiar succession of phase transitions, which is a unique feature of this model, absent in analogous simpler ones.[9,10]

To proceed, let us see in detail the general features of the loci following Eq. (A3). The zeros are eight in number, but each of them is double, so that we have only four distinct values, which are the roots of the equation

$$1-\left[-\frac{1}{2}\frac{\gamma}{\beta}\right]H^2\frac{(Q^2-\frac{1}{2}QJ+Z^2/4)}{(Q^2-Z^2/4)^2}=0 \ , \tag{A4}$$

$Q_k(H)$, $k=1,\ldots,4$, indicates the zeros. The structure of Eq. (A4) is the same than that of the characteristic equation for the planar configurations, Eq. (14), but the field-dependent gain here can have either sign, depending on the interaction parameters.

The root locus of Eq. (A4) is shown, for positive and for negative gain, in Fig. 7. If $\gamma\beta>0$, all zeros are complex at any nonzero field, while if $\gamma\beta<0$, two of them are always real, the other ones becoming complex for fields exceeding the "branching field" H_{bQ} to be calculated by substituting into Eq. (A4) the solution of the "branching equation"[9,14]

$$16\lambda^3-12\lambda^2J+12\lambda Z^2-JZ^2=0 \ .$$

The poles of Eq. (A3) are all real and field independent. Two of them have each quadrupole multiplicity and opposite values $P_2=+Z/2$, $P_3=-Z/2$, while the other one, P_1, already cited above, is simple, so that the real values of λ lay only on one side of it.

Now we can come back to the relations (A2). A necessary condition for λ^{ax} or λ^{con} (the suffixes obviously indicate which configuration we are referring to) going continuously into λ_c as H increases, is that no singularity happens to fall in between the zero-field values of them and λ_c, so that the whole interval of the real axis belongs to one and the same real branch for any locus to be considered. As P_2 lays always to the right of $\lambda^{ax}(0)$ (indeed, $t+Z<0$ in the

axial phase existence range) but it coincides with $\lambda^{con}(0)$, the only intermediate pole could be P_1. It is, however, immediate to show that the inequality expressing that occurrence

$$[P_1-\lambda^{ax,con}(0)](P_1-\lambda_c)<0$$

is never verified. Could a zero be the intermediate singularity? Surely not if $\gamma\beta>0$, because then they are all complex for nonzero fields. If $\gamma\beta<0$, there is one real zero moving from P_2 towards $+\infty$ as H increases. Its motion is described by Eq. (A4) (with positive gain), while the position of λ_c follows from Eq. (14) with $H=H_c$. Now, these equations differ only in the structure of the gain parameters. When $H=H_c$, the position of the zero will correspond to the gain value $(-\gamma/2\beta)H_c^2$, and that of λ_c to $H_c^2/16$. If the former value is greater than the latter, the zero must surpass $\lambda^{ax}(H)$ or $\lambda^{con}(H)$ at a lower value of H, when they had not yet reached λ_c. As a consequence, a second-order transition becomes impossible. A necessary condition for a continuous transition is then $(-\gamma/2\beta)<\frac{1}{16}$ which is equivalent to Eq. (A2). A further condition can be obtained by developing the equation $m_{\pm z}(H_c)=0$, yielding $\beta=-4\gamma+t/16+\lambda_c/8$. From the locus of Eq. (14), referring to the planar phase, one sees that $\lambda^p(H)\geq Z/2$. Then also $\lambda_c>Z/2$, implying that the minimum value for β is $\beta=-4\gamma+p/16$. Below the line of the (p,β) plane defined by the relation above, the transition is surely first order. This is a requisite more stringent than Eq. (A2) if $\gamma>0$ and $p>-64\gamma$, or $\gamma<0$ and $p<-64\gamma$.

All these considerations refer to the possibility of a given nonplanar phase, stable at $H=0$, making a transition to the planar phase stable at high fields. No possible transitions between two nonplanar phases was considered up to now. But consideration of the root loci of Eq. (A3) shows that also this type of transition may happen, and that it is always a discontinuous one. If $\gamma>0$, $p<0$, $-4\gamma+p/16>\beta>p/4-4\gamma$ or $-4\gamma+p/16>\beta>-2(\gamma/p)^{1/2}$, the axial phase is stable at $H=0$, but cannot have a continuous transition to the planar configuration. The loci of Eq. (A3), having positive gain, are real only for $\lambda\geq P_1$, and we have $P_1>P_2$. One zero, Q_1 say, is always real and moves from P_2 towards $+\infty$. $\lambda^{ax}(H)$ starts at $\lambda^{ax}(0)=-t/2$, which is greater than P_1 (as $\gamma>0$). For low fields, the loci appear as in Fig. 8(a): no singularity exists between P_1 and $\lambda^{ax}(0)$, nor on the right of P_1. As $\beta<-4\gamma$, $\lambda_c<\lambda^{ax}(0)$, and $\lambda_c>P_1$. Then $\lambda^{ax}(H)$, moving towards λ_c, decreases its value. At a certain value of H, H_1 say, Q_1 overtakes P_1, and a dramatic change occurs in the locus, which assumes the shape of Fig. 8(b). This is an example of the case where an infinitesimal change of H, deplacing Q_1 from the left to the right of P_1, changes discontinuously the topology of the locus. Now a branching point is present to the right of Q_1, and the real axis to the right of Q_1 represents the high-gain section of the locus branches starting from P_2 and ending either at infinity or in Q_1. As H increases, Q_1 moves to the right, and reaches λ_c before

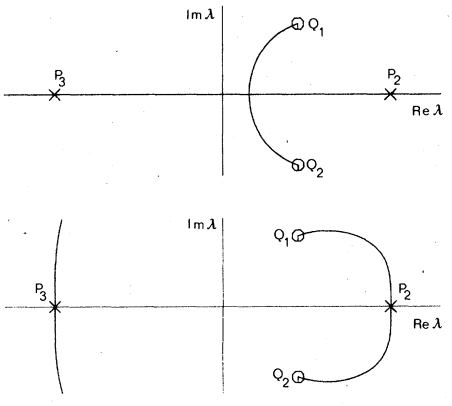

FIG. 7. Root locus of Eq. (A4) for positive (top) and negative (bottom) gain. Circles indicate the zeros, crosses, the poles. J is assumed positive. For ease of comparison, the poles are labeled as in the following Fig. 8, because their values are identical in the two cases. No such relation, on the contrary exists for the labels of the zeros.

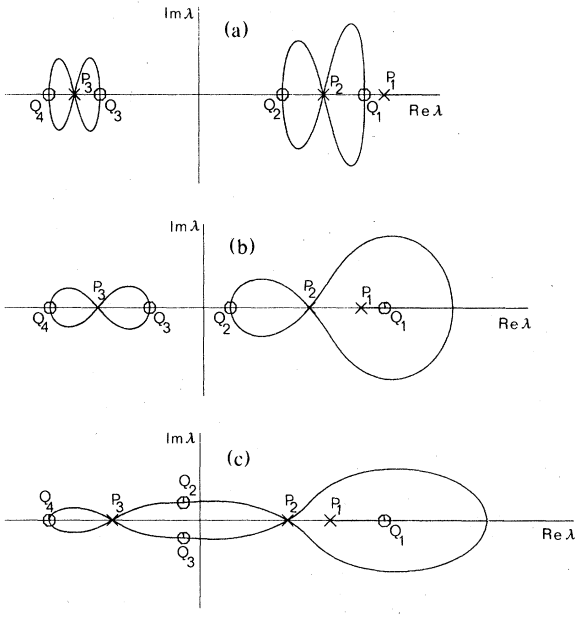

FIG. 8. (a)–(c) Loci of Eq. (A3) for positive gain, and for three values of H. From top to bottom, H is: lower than H_1, intermediate between H_1 and H_{bQ}, and greater than H_{bQ} (see the text for the definitions of H_1 and H_{bQ}). The values of the parameters are $Z=1.118$, $K_2=K_z=-1.51$, $\beta=-0.84$, $\gamma=0.159$, $H=0.7/1.5/2.3$.

$\lambda^{ax}(H)$, as $\beta > -8\gamma$. If we denote by $g_b(H)$ and $g_{ax}(H)$ the gain values corresponding, respectively, to the branch point $\lambda_b(H)$ (depending on H through the field dependence of the zeros), and to $\lambda^{ax}(H)$, nothing interesting happens if $|g_{ax}| > |g_b|$. As the zero moves towards $+\infty$, the gain relative to any real point to its right increases in absolute value, and when H becomes greater than the value H_2 for which $|g_{ax}| = |g_b|$, λ^{ax} cannot stay longer on the same branch as before, because, on that branch, g_{ax} corresponds now to a complex value. The value of λ corresponding to a physical configuration has to be real, and the only possibility is that it falls between P_1 and Q_1, on a point which, on that branch, corresponds to the same gain g_{ax}. Indeed, the gain cannot vary discontinuously, while the root value can.

So the physical λ will have a value lower than before by a finite amount: as a consequence, the resulting m_{+x} will increase discontinuously (indeed $\partial m_{+x}/\partial\lambda < 0$) and we will observe a first-order transition. Which configuration will be realized? Two cases are possible: either Q_1 as surpassed λ_c for $H = H_2$, or it is still to the left of λ_c. In the first case, the transition will be to a planar configuration, with a new λ greater than λ_c; it may be that the conical phase also appears, but as a metastable state. In the second case, the conical phase (impossible at $H = 0$, but not for $H \neq 0$) will be realized after the first-order transition, and it will perform a second-order transition to the planar phase at $H = H_c$ (as $\beta > -8\gamma$). We discover then the possibility of a sequence of phase transitions of different types, the one of first order taking place between two nonplanar configurations, an occurrence excluded in simpler models.[9,10] This result could not be arrived at, we believe, just by examining Eq. (20) or the expression of the energy of the system. This justifies the use of the root-locus technique, which also allows a precise determination of the fields H_1 and H_2, by substituting into Eq. (A4) P_1 and λ_c for Q_1.

APPENDIX B: DISCONTINUITY OF THE SUSCEPTIBILITY AT THE SECOND-ORDER TRANSITION

It is not difficult to obtain the explicit expression of $\Delta\chi_c$ defined in Sec. VII. One has essentially to work out the $\lim_{H\to H_c} d\lambda/dH$ from Eqs. (14) and (20), for the nonplanar and the planar configurations. The final result is [we put $f = H/(4\lambda^2 - Z^2)$ for brevity]

$$\Delta\chi_c = -\left[\frac{2f^2}{H}\right](4\lambda^2 - 2\lambda J + Z^2)\left[\frac{d\lambda^{np}}{dH} - \frac{d\lambda}{dH}\right]$$

$$= \frac{2f^3(4\lambda^2 - 2\lambda J + Z^2)\epsilon/[\beta^2 + 4\gamma(2\lambda + t)]^{1/2}}{A(\lambda,H)B(\lambda,H)} ,$$

where

$$A(\lambda,H) = 8\lambda f^3(4\lambda^2 - 2\lambda J + Z^2) - Hf^2(4\lambda - J) ,$$

$$B(\lambda,H) = 8\lambda f^3(4\lambda^2 - 2\lambda J + Z^2) - Hf^2(4\lambda - J) + H\epsilon/[\beta^2 + 4\gamma(2\lambda + t)]^{1/2} ,$$

and $\epsilon = +1$ if "np" means "conical", but $\epsilon = |\beta|/\beta$ if "np" means "axial." $A(\lambda,H)$ is always positive, being proportional to $d\lambda^p/dH$. $B(\lambda,H)$ has the sign of $d\lambda^{np}/dH$, so it is positive if np = conical, in which case also $\epsilon = +1$ and $\Delta\chi_c$ cannot be negative. If np = axial, one must distinguish: when γ is positive, a continuous transition, requiring $\beta < -8\gamma < 0$ implies also $\lambda_c < \lambda^{ax}(0)$, because the opposite is true only if $\beta > -4\gamma$. It follows that $d\lambda^{ax}/dH$ is negative, but then also ϵ is, and the overall $\Delta\chi_c$ is positive. If γ is negative, $\beta > -8\gamma$ implies also $\lambda^{ax}(0) < \lambda_c$ and $d\lambda^{ax}/dH > 0$ as well as ϵ, so that again $\Delta\chi_c$ turns out to be positive.

[1] J. Smit and H. P. Wijn, *Ferrites* (Wiley, New York, 1959).
[2] M. I. Darby and E. D. Isaac, IEEE Trans. Magn. 10, 259 (1974).
[3] K. P. Belov *et al.*, Bull. Acad. Sci. U.S.S.R. Phys. Ser. 34, 981 (1971).
[4] L. N. Koroleva and L. P. Mitina, Phys. Status Solidi (a) 5, K55 (1961).
[5] G. Albanese *et al.*, Appl. Phys. 7, 227 (1975).
[6] B. R. Morrison, Phys. Status Solidi (b) 59, 581 (1973).
[7] T. Sugiura *et al.*, J. Phys. Soc. Jpn. 38, 365 (1975).
[8] C. W. Fairall and J. A. Cowen, Phys. Rev. B 2, 4636 (1970).
[9] M. Acquarone and S. Rinaldi, J. Phys. Chem Solids 39, 333 (1978).
[10] M. Acquarone, J. Phys. C 12, 1373 (1979).
[11] I. S. Jacobs *et al.*, Int. J. Magn. 1, 193 (1971).
[12] N. Yamashita, J. Phys. Soc. Jpn. 32, 610 (1972).
[13] J. Berger and R. M. Hornreich, J. Phys. Chem. Solids 34, 2011 (1973).
[14] See, for instance: L. Dale Harris, *Introduction to Feedback Systems* (Wiley, New York, 1961).
[15] J. N. McElearney and S. Merchant, Phys. Rev. B 18, 3612 (1978).
[16] L. J. de Jongh and A. R. Miedema, *Experiments on Simple Magnetic Model Systems* (Taylor and Francis, London, 1974).
[17] Y. Tsuchida *et al.*, Prog. Theor. Phys. 56, 1011 (1976).
[18] H. Puszkarski and P. E. Wigen, Phys. Rev. Lett. 35, 1017 (1975).
[19] T. Siskens *et al.*, Physica (Utrecht) 79A, 259 (1975).
[20] V. I. Limar and Y. G. Rudoi, Theor. Math. Phys. 34, 137 (1978).
[21] V. I. Ozhogin, IEEE Trans. Magn. 12, 19 (1979).

[22]U. Enz, J. Appl. Phys. 32, 22s (1961).
[23]A. Yoshimori, J. Phys. Soc. Jpn. 14, 807 (1959); T. A. Kaplan, Phys. Rev. 116, 888 (1959); J. Villain, J. Phys. Chem. Solids 11, 303 (1959); D. H. Lyons and T. A. Kaplan, Phys. Rev. 120, 1580 (1960); D. H. Lyons, *ibid.* 132, 122 (1963); T. Nagamiya, Solid State Phys. 20, 305 (1967).
[24]Similar structures, also observed in substituted M and W hexaferrites, will not concern us here, because in those crystals a different orientation of the DM vector would have to be considered.
[25]T. M. Perekalina *et al.*, Sov. Phys. JETP 25, 266 (1967) [Zh. Eksp. Teor. Fiz. 52, 409 (1967).
[26]V. A. Sizov *et al.*, Sov. Phys. JETP 26, 736 (1968) [Zh. Eksp. Teor. Fiz. 53, 1256 (1967)].
[27]M. I. Namtalishvili *et al.*, Sov. Phys. JETP 35, 370 (1972) [Zh. Eksp. Teor. Fiz. 62, 701 (1972)].
[28]T. M. Perekalina *et al.*, Sov. Phys. JETP 31, 440 (1970) [Zh. Eksp. Teor. Fiz. 58, 821 (1970)].
[29]D. G. Sannikov and T. M. Perekalina, Sov. Phys. JETP 29, 396 (1969) [Zh. Eksp. Teor. Fiz. 56, 730 (1969)].
[30]T. M. Perekalina *et al.*, Sov. Phys. JETP 30, 410 (1970) [Zh. Eksp. Teor. Fiz. 57, 749 (1969)].
[31]R. A. Sizov, Sov. Phys. Solid State 16, 57 (1974) [Fiz. Tverd. Tela 16, 98 (1974)].
[32]Y. Kitano and T. Nagamiya, Prog. Theor. Phys. 31, 1 (1964).
[33]This picture emerges from the data of Refs. 26 and 31, but this is not the opinion of the authors of those papers. Referring to the theory of U. Enz (Ref. 22), they state that the angle ϕ increases with H along the plateau, reaching the value π at the transition to the planar configuration. Then one would expect m_{+x} to vanish at the transition. In our opinion they misinterpret the theory of Ref. 22, neglecting the field dependence of the amplitude of ϕ in the "oscillatory" state. This dependence results in a decreasing amplitude with increasing field. Neutrons measure a different quantity, namely, the variation with the field of the spatial period of the magnetic structure. The data of Refs. 26 and 31 then show that every other moment stays parallel along the chain, so supporting a two-sublattice picture.
[34]H. B. Callen and E. Callen, J. Phys. Chem Solids 27, 1271 (1966).
[35]G. Asti and S. Rinaldi, in *Magnetism and Magnetic Materials—1976,* edited by J. J. Becker and G. H. Lander, AIP Conf. Proc. No. 34 (AIP, New York, 1976), p. 214.
[36]G. Albanese and A. Deriu (private communication).